Numerical Modeling of Hydrothermal System in the Western Region of Kirishima Volcano in Kagoshima Prefecture, Japan

Tabuchi Amane[1], Nishijima Jun[2]

[1] Cooperative Program for Resources Engineering, Graduate School of Engineering, Kyushu University,

744, Motooka, Nishi-ku, Fukuoka 819-0395, Japan

[2] Department of Earth Resources Engineering, Faculty of Engineering, Kyushu University,

744, Motooka, Nishi-ku, Fukuoka 819-0395, Japan

tabuchi.amane.652@s.kyushu-u.ac.jp

Keywords: *Kirishima Volcano, hydrothermal system, conceptual model, numerical model*

ABSTRACT

Well-developed geothermal areas exist in the Ogiri and Shiramizugoe areas, located in the western part of the Kirishima Volcano. As understanding the hydrothermal system is extremely important for sustainable geothermal development, numerical models of hydrothermal systems under natural conditions have been developed to investigate both areas. However, the reproduction of pressure profiles in this area remains an issue, and one possible reason is the existence of an impermeable layer between the Ogiri and Shiramizugoe areas. Thus, in this study, we classified the part of the NW fault between the Ginyu and Shiramizugoe faults that are distributed in a high-density area, estimated from the airborne gravity anomaly method survey (Nishijima, 2016). We created a model wherein the Ogiri and Shiramizugoe areas are independent of each other by the impermeable layer owing to low permeability. Simulations were conducted using HYDROTHERM-Version 3.2 (Kipp et al., 2008) to investigate the hydrothermal system.

The simulation results indicated that the calculated pressure profiles of the wells located in the target area were approximately 5 MPa higher than the measured values. As all voids in this model were saturated with water up to the surface block, the differences between the calculated and actual groundwater levels can be attributed to the fact that the calculated pressure values exceed the measured values. Therefore, when the influence of the groundwater surface is corrected using the pressure determined from the simulation, the pressure difference between the Ogiri and Shiramizugoe areas can be reproduced. Therefore, we developed a model that can explain the temperature and pressure in this area by reducing the permeability of the NW fault distributed in the high-density area between the Ogiri and Shiramizugoe areas.

1. INTRODUCTION

Since the 2011 off the Pacific coast of Tohoku Earthquake, renewable energy use has garnered increasing attention in Japan. The Japanese government has set the goal of introducing an installed capacity of 1.48 million kW of geothermal power by 2030 to achieve carbon neutrality by 2050. Thus, further promotion of geothermal development as a new baseload power generation source is needed.

A new geothermal development project is planned in the western part of the Kirishima Volcano in Kagoshima Prefecture, southern Kyushu. In the Ogiri area, the Ogiri Power Plant began operation in March 1996 and has been in operation for 28 years. Various surveys have been conducted by the national government and private companies in the Shiramizugoe area, which is located southeast of Ogiri. Promising geothermal resources at higher temperatures than those in the Ogiri area have been identified, and a new survey by Nittetsu Mining Co. was announced for 2023. Location of the geothermal field in the western region of Kirishima Volcano is shown in Fig. 1.

An accurate understanding of hydrothermal systems and resource assessment is necessary for sustainable geothermal development. Modeling of hydrothermal systems and numerical simulations of the natural state were used to understand the hydrothermal system. In this study, we conducted a natural state simulation of the western Kirishima Volcano area using HYDROTHERM-Version 3.2 (Kipp et al., 2008) to investigate the hydrothermal system in the western Kirishima Volcano area.

2. GEOLOGICAL SETTING

Kirishima Volcano is a group of volcanoes straddling the border between Miyazaki and Kagoshima prefectures. It comprises more than 20 stratovolcanoes and pyroclastic hills, including Mt. Iwo-yama, Onami-ike, and Shinmoe-dake. Kirishima Volcanoes, including the Ogiri area, is located on the volcanic front where the Philippine Sea Plate subducts beneath the Eurasian Plate and is the northern end of the 20-km wide Kagoshima Graven, which extends from NNE to SSE. The geothermal area in the western part of the Kirishima

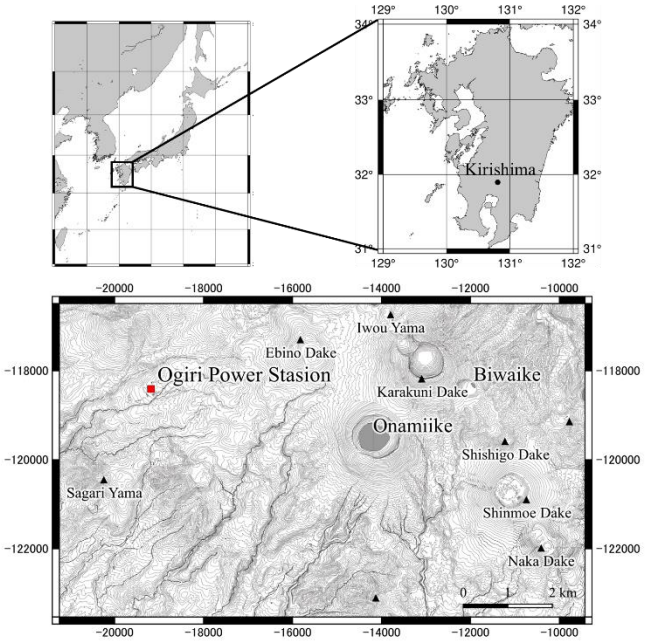

Figure 1: Location of the geothermal field in the western region of Kirishima Volcano, Kyushu Island, Japan.

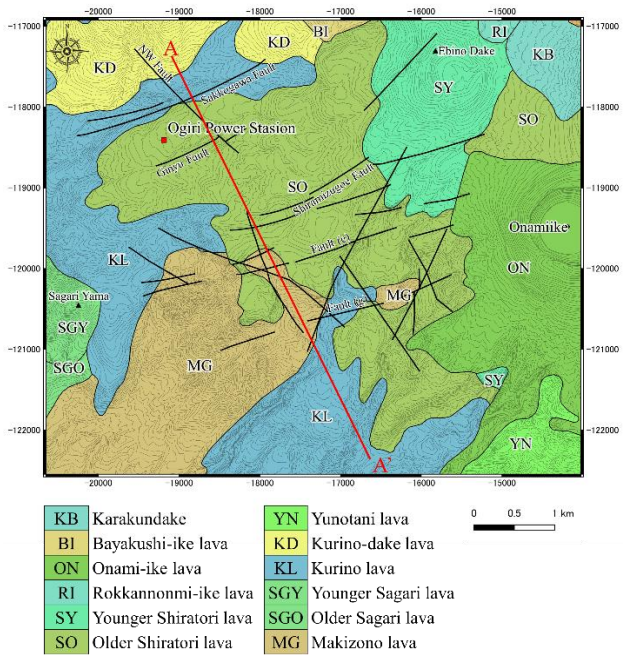

Figure 2: Geological map and fault locations of western part of Kirishima Volcano (modified from NEDO (2003)). The red line indicates the location of the cross section of the conceptual model (Fig. 4).

Volcano comprises basement rocks from the Shimanto Formation of the Mesozoic Cretaceous to Cenozoic Paleogene period, which is widely distributed in the outer belt of southwestern Japan. The volcanic rocks and lake sediments of the Quaternary Pleistocene have widely overlaid basement rocks. The Ito Ignimbrite (Shirasu), which erupted during the formation of the Aira caldera in the Late Pleistocene, is widely distributed around the Kirishima Volcano. The formations exposed around the Ogiri area are Makizono and Sagari lava of the Kakuto andesite and Kurino lava, Takahara gravel, Kurino-dake lava, Older Shiratori lava, Younger Shiratori lava, Rokkannon-ike lava, Onami-ike lava, and Karakuni-dake lava of the Old to Middle Kirishima volcanic rocks (Goko, 2020). The geological map is shown in Fig. 2.

Numerous faults are distributed in the western part of the Kirishima Volcano. The surface fracture system in this area is characterized by faults and lineaments in the NW-SE and ENE-WSW directions (Fig. 2). Based on the stress fields determined from microseismic data from Kirishima Volcano, including the Ogiri area, Kirishima Volcano is present in a stress field with a tension axis in the NW-SE direction (Ida et al., 1986; Kagiyama et al., 1990). Thus, open-type fractures have been developed in the ENE-WSW system, and these fractures are expected to provide a pathway for geothermal fluids. There are numerous alteration zones at the surface, and the distribution of alteration zones corresponds well with that of the faults.

3. CONCEPTUAL MODEL

A conceptual model of the hydrothermal system is shown in Figs. 3 and 4. At Kirishima Volcano, magneto telluric (MT) surveys and InSAR analysis have been conducted to understand crustal deformation associated with volcanic activities at Mt. Iwo-yama and Mt. Shinmoedake (Yoshinaga et al., 2023). According to the results, we estimated the heat source of the geothermal system in the western part of Kirishima Volcano. Magma is supplied from a magma reservoir estimated at a depth of 10 km, immediately below Mt. Iwo-yama (Magma Source A in Fig. 3) to a magma reservoir estimated to be 2 km west of Onami-ike at a depth ranging from approximately 6 to 7 km (Magma Source B in Fig. 3). The hydrothermal system in the western part of Kirishima Volcano was formed by Magma B as a heat source.

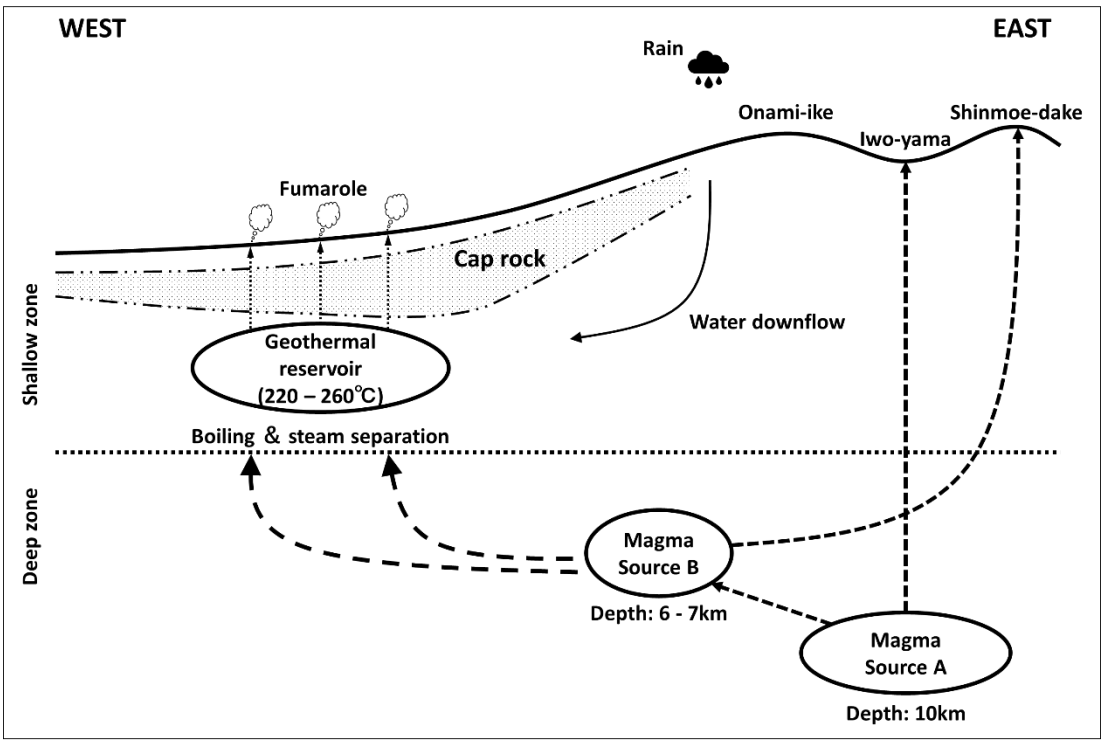

Figure 3: Conceptual model of the geothermal system of the EW cross section in the western part of Kirishima Volcano determined from geochemical and geophysical analyses.

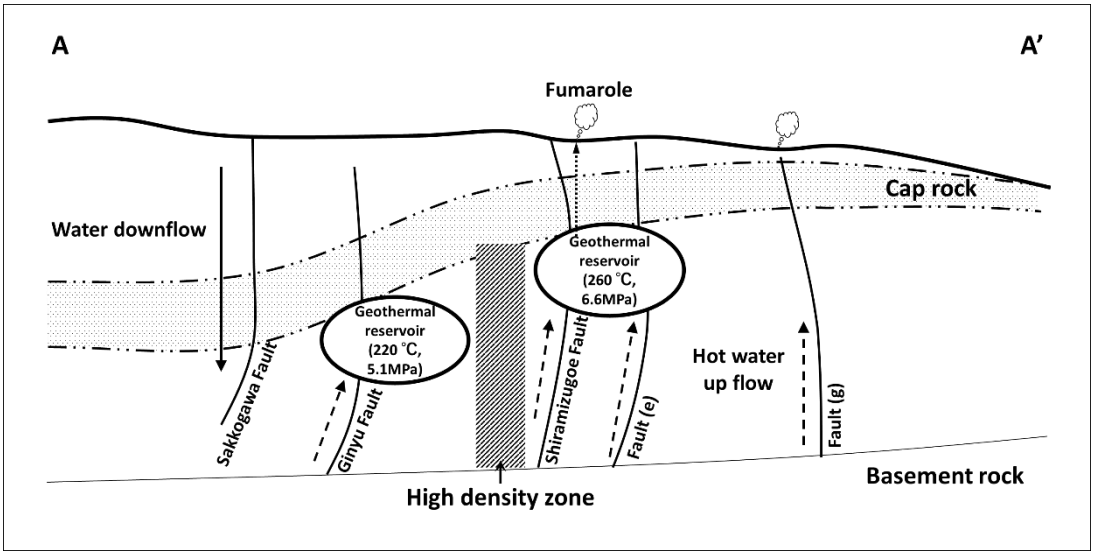

Figure 4: Conceptual model of the geothermal system of the A-A' cross section in the western part of Kirishima Volcano determined from geochemical and geophysical analyses.

The main recharge fault is the Sakkogawa fault located north of the hydrothermal system in the Ogiri area. According to Goko (2000), the temperature distribution in wells located around the Sakkogawa fault shows low temperatures extending to lower elevations. Meteoric water is heated by magma and supplied to reservoirs as geothermal fluids. High-temperature geothermal fluids rise to the shallow part through fractures in the Ginyu and Shiramizugoe faults, which have high permeabilities. Therefore, geothermal reservoirs are formed along the Ginyu fault in the Ogiri area, with the Sakkogawa fault as the recharge zone, and along the Shiramizugoe fault and fault (e) in the Shiramizugoe area.

Nishijima (2016) conducted three-dimensional subsurface density structure modeling of the subsurface using data from an airborne gravity gradiometry data conducted by the Japan Oil, Gas and Metals National Corporation (JOGMEC) for the western area of Kirishima Volcano. The high temperature at -300 m a.s.l. was distributed around the eastern side of the high-density area between the Ogiri and Shiramizugoe areas. The reservoir pressure was different in the Ogiri (5.1 MPa) and Shiramizugoe (6.6 MPa) areas. The distribution of the high-density area corresponded to the steep pressure-change area between the Ogiri and Shiramizugoe areas. Therefore, dense rocks with few pores are known to be distributed in the high-density area between the Ogiri and Shiramizugoe areas, forming an impermeable layer separating the Ogiri and Shirazugoe reservoirs.

According to Goko (2000), an impermeable layer is formed by clay minerals, mainly smectite, that fractures rocks at elevations between 200 and 500 m in the target area.

4. NUMERICAL SIMULATION

To understand the hydrothermal system in the western region of Kirishima Volcano, we conducted numerical simulations using HYDROTHERM-Version 3.2 (Kipp et al., 2008). HYDROTHERM can simulate the model heat energy transfer and hydrothermal flow systems.

4.1 Analysis area

The analysis area is 6 × 6 km horizontally and -1.2 to 1.5 km vertically to include the Ogiri and Shiramizugoe areas. The mesh comprises 100 m × 60 grid blocks in the horizontal direction (*i*, *j* index) and 50 m × 55 grid blocks in the vertical direction (*k* index). The dimensions of the buffer area were 200, 300, 400, 500, and 50 m, in the order closest to the analysis area. The analysis area was tilted 20° to the west from the N-S direction to linearly reproduce the ENE-WSW fault that dominated the target area. The study area is shown in Fig. 5.

The topography was approximated to the ground surface. The subsurface structure was reproduced based on geological, geophysical, and logging data integrated using geographic information systems (GIS). The model comprises 23 types of rocks: basement rock, five volcanic rocks, low-permeability zone, high-density zone, and seven faults and their low-permeability zones (Table 1). The parameters of the volcanic rocks were determined from measurements of rock samples

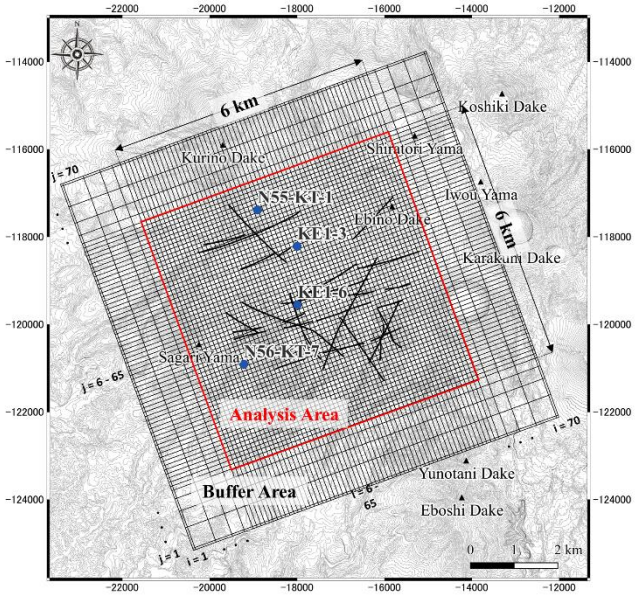

Figure 5: Plan view of the "study area" and conceptional grid. The black lines indicate the distribution of faults on the ground surface. The blue points represent the location of wells used to fit the simulation results.

Table 1: Rock parameters for the numerical simulation

	Porosity [-]	Permeability in X [m^2]	Permeability in Y [m^2]	Permeability in Z [m^2]	Thermal conductivity [$W\ m^{-1}\ K^{-1}$]	Specific heat capacity [$J\ kg^{-1}\ K^{-1}$]	Density [$kg\ m^{-3}$]
Basement rock	0.04	2.5×10^{-16}	2.5×10^{-16}	2.5×10^{-16}	2.75	834	2620
Volcanic rock 1	0.11	2.5×10^{-16}	2.5×10^{-16}	2.5×10^{-16}	1.89	825	2410
Volcanic rock 2	0.18	1.0×10^{-15}	1.0×10^{-15}	1.0×10^{-15}	1.59	817	2070
Volcanic rock 3	0.12	1.0×10^{-15}	1.0×10^{-15}	1.0×10^{-15}	1.72	837	2360
Volcanic rock 4	0.10	5.0×10^{-15}	5.0×10^{-15}	5.0×10^{-15}	1.59	834	2390
Volcanic rock 5	0.06	5.0×10^{-15}	5.0×10^{-15}	5.0×10^{-15}	1.72	857	2560
Low-permeability zone	0.01	1.0×10^{-20}	1.0×10^{-20}	1.0×10^{-20}	1.68	843	2437
High-density zone	0.11	1.0×10^{-18}	1.0×10^{-18}	1.0×10^{-18}	1.66	834	2400
Fault 1	0.11	1.0×10^{-14}	1.0×10^{-13}	1.0×10^{-14}	1.66	834	2358
Fault 1*	0.01	1.0×10^{-18}	1.0×10^{-17}	1.0×10^{-18}	1.68	843	2437
Fault 1 (High-density zone)	0.11	1.0×10^{-18}	1.0×10^{-18}	1.0×10^{-18}	1.66	834	2400
Fault 2	0.11	1.0×10^{-12}	1.0×10^{-13}	1.0×10^{-12}	1.66	834	2358
Fault 2*	0.01	1.0×10^{-16}	1.0×10^{-17}	1.0×10^{-16}	1.68	843	2437
Fault 3	0.11	1.0×10^{-12}	1.0×10^{-13}	1.0×10^{-12}	1.66	834	2358
Fault 3*	0.01	1.0×10^{-16}	1.0×10^{-17}	1.0×10^{-16}	1.68	843	2437
Fault 4	0.11	1.0×10^{-14}	1.0×10^{-15}	1.0×10^{-14}	1.66	834	2358
Fault 4*	0.01	1.0×10^{-17}	1.0×10^{-18}	1.0×10^{-17}	1.68	843	2437
Fault 5	0.11	1.0×10^{-14}	1.0×10^{-15}	1.0×10^{-14}	1.66	834	2358
Fault 5*	0.01	1.0×10^{-17}	1.0×10^{-18}	1.0×10^{-17}	1.68	843	2437
Fault 6	0.11	1.0×10^{-13}	1.0×10^{-14}	1.0×10^{-13}	1.66	834	2358
Fault 6*	0.01	1.0×10^{-18}	1.0×10^{-19}	1.0×10^{-18}	1.68	843	2437
Fault 7	0.11	1.0×10^{-13}	1.0×10^{-14}	1.0×10^{-13}	1.66	834	2358
Fault 7*	0.01	1.0×10^{-17}	1.0×10^{-18}	1.0×10^{-17}	1.68	843	2437

*Low-permeability zone located at each fault.

collected in the field. Based on the density structure estimated from an airborne gravity anomaly survey (Nishijima, 2016), areas with densities above 2350 kg/m^3 were designated as high-density zones (density of 2400 kg/m^3). The impermeable layer separating the Ogiri and Shiramizugoe areas was reproduced by reducing the permeability of the NW fault in this region. HYDROTHERM can only handle porous models; thus, the faults were reproduced as a highly permeable zone. Anisotropy was applied to the horizontal permeability to reproduce differences in the strike of the fault. We adjusted the permeability of the fault blocks until a reasonable fit was achieved between the observed and simulated temperature and pressure profiles in the wells located in the analysis area. The other parameters were considered as the average values for the five volcanic rocks.

4.2 Boundary and initial conditions

The calculation period was set to 100,000 years based on the active period of Onami-ike, where the magma reservoir, which is the heat source of this geothermal system, was located. At this point, they were assumed to represent natural state conditions.

The boundary conditions of the ground surface were permeable with constant temperature and pressure in the area, and the bottom was impermeable with a crustal heat flux of 150 mW/m^2. The eastern side was set as an impermeable boundary owing to the watershed, whereas the other sides were open boundaries with constant temperature and pressure. As the magma reservoir in the eastern part of the study area was assumed to supply hydrothermal fluids through the fracture system, hydrothermal fluids were allowed to flow from four locations on the eastern side of the fault basement (Fig. 6). The temperature and flow rate for each heat source are presented in Table 2.

Table 2: Characteristics of the heat sources

	Temprature (°C)	Flow rate ($kg\ s^{-1}$)
Heat source 1	250	10.0
Heat source 2	260	20.0
Heat source 3	290	10.0
Heat source 4	300	5.0

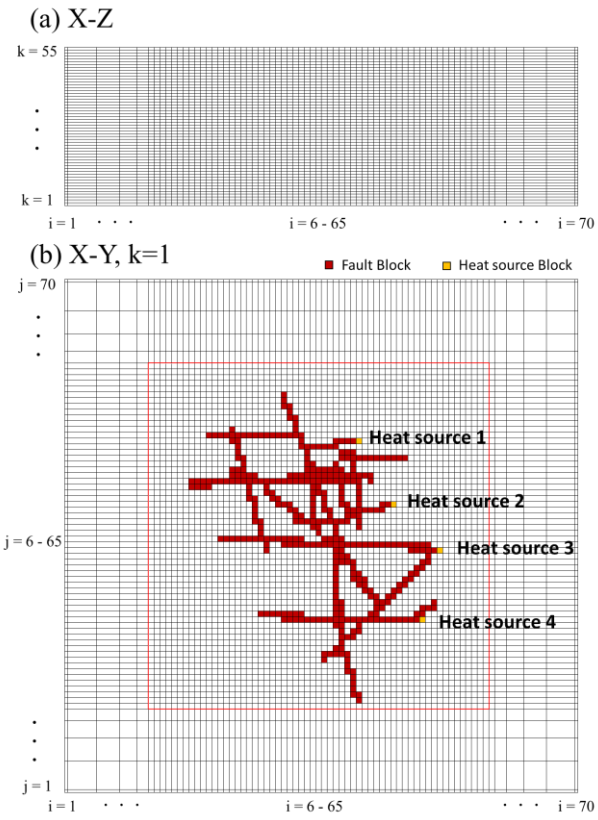

Figure 6: Block division and heat source block at the bottom.

Considering the initial conditions, the surface temperature was set to 15.9 ℃, which is the average air temperature in the target area, and the subsurface temperature was calculated using a temperature gradient of 30 °C/km, which is the average for non-volcanic regions. The initial pressure was the depth hydrostatic pressure of 0.1013 MPa at the ground surface.

5. RESULTS

5.1 Pressure profiles

The observed and calculated pressures in wells located in the target area were compared. The pressure profile was the reservoir pressure at the feed point of each well, and the pressure calculation value was the center pressure of the block where the feed point of each well was located. The calculated pressure exceeded that measured in all the wells. The measured pressure in the Ginyu fault at -300 m was 1.6 MPa lower than that in the Shiramizugoe area, but the calculated pressure in the Ginyu area was higher than that in the Shiramizugoe area.

In this model, the pressure is calculated by providing the hydrostatic pressure up to the surface block. Thus, the model considered that this caused a pressure difference of approximately 5 MPa between the calculated and measured pressures. The elevation of the permeable layer north of the Ginyu area was lower than that of the Shiramizugoe area, and the groundwater surface elevation was lower. Thus, we considered that the Ginyu area was more strongly affected by the groundwater surface elevation. Therefore, we examined a model wherein the effect of the groundwater table was corrected by removing the extra pressure at the top of the well from the calculated pressure (Fig. 7).

Consequently, the calculated pressure values in both the Ginyu and Shiramizugoe areas decreased and approached the measured values. In particular, the pressure in the Shiramizugoe area decreased by approximately 2 MPa at an elevation of 200 m, which approached the observed pressure gradient. The decrease in pressure in the Ginyu area also enabled the reproduction of the pressure difference between the Ginyu and Shiramizugoe areas. Therefore, we believe that we can reproduce the pressure trends in the Ginyu and Shiramizugoe areas by considering the influence of the groundwater surface. The simulation of a model that includes unsaturated zones will be the subject of future work.

5.2 Temperature profiles

We assessed the validity of the model by comparing the simulated temperature values with temperature profiles (Fig. 8). The simulation results showed that the simulated temperature values approximately matched the measured ones in several wells located in the eastern and central parts of the analysis area (N55-KT-1, KE1-3, and KE1-6). N55-KT-1 is located north of the Sakkogawa fault. The temperature was below 100 ℃ at an elevation of 0 m, indicating the inflow of surface water. KE1-3 and KE1-6 are located on the Ginyu and Shiramizugoe faults, respectively. From the temperature profiles of KE1-3 and KE1-6, a high temperature gradient was observed at elevations between 500 and 0 m for KE1-3 and 800 and 200 m for KE1-6. This temperature gradient was characterized by a cap rock. Furthermore, the temperature remained constant at elevations below these points. Conversely, in some wells located in the southwestern part of the analysis area, such as N56-KT-7, the simulated values were larger than the measured values, and the temperature profiles did not reproduce the temperature distribution, indicating the inflow of surface water.

Based on these results, we created a model that can calculate temperature and pressure, although this is not a perfect reproduction. Therefore, this model is reasonable and can

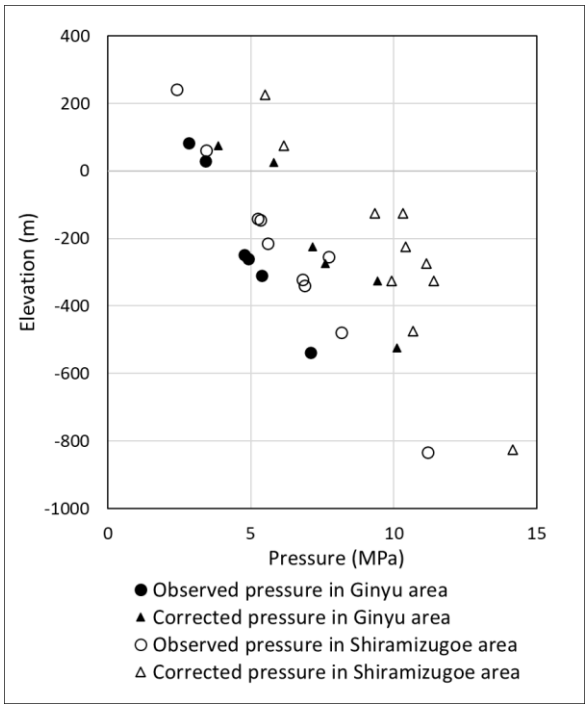

Figure 7: Pressure profile of the feed points of each well, comparison between observed and simulated results. Corrected for the effect of groundwater level on wellbore pressure.

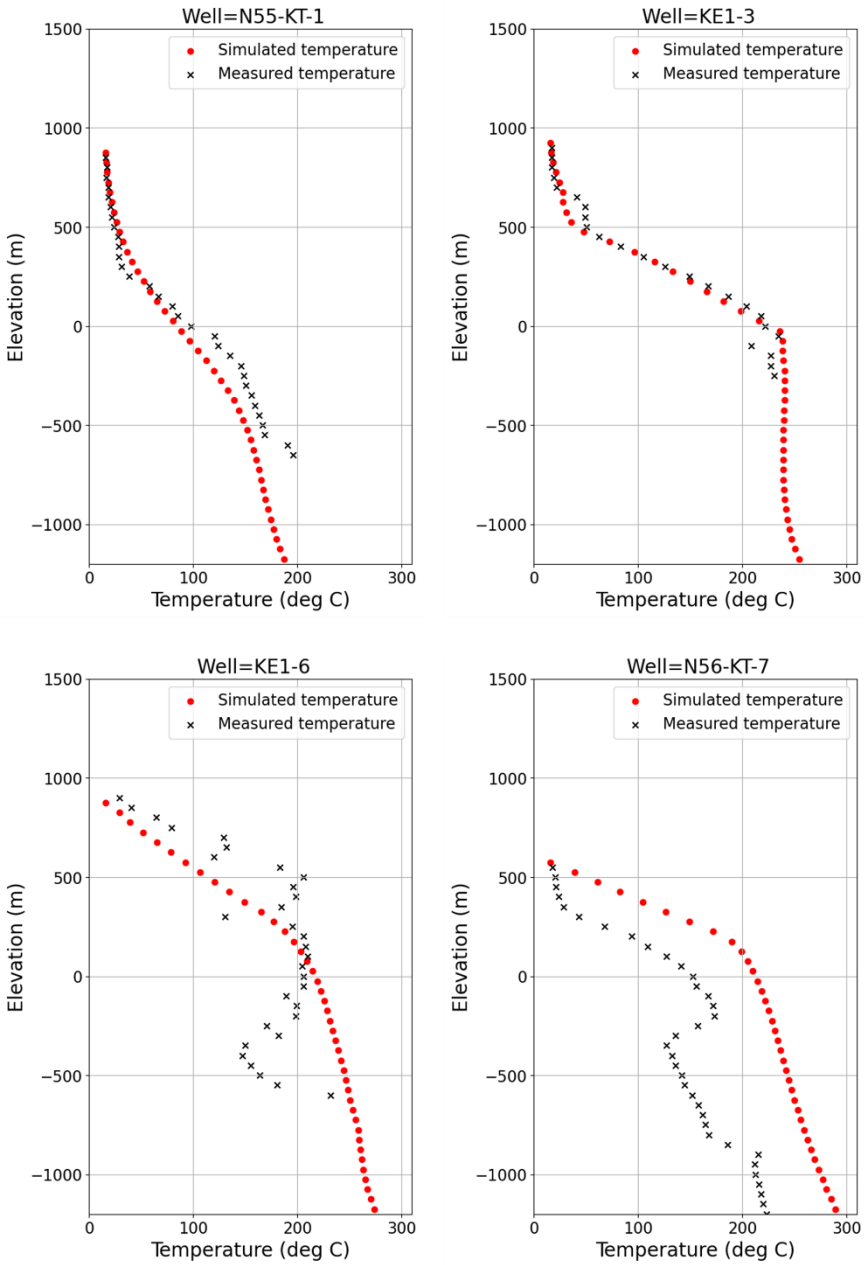

Figure 8: Temperature profile of N55-KT-1, KE1-3, KE1-6, and N56-KT-7, comparison between measured and simulated

reproduce the impermeable layer between the Ogiri and Shiramizugoe areas owing to the lower permeability of the NW fault distributed in the high-density area between these areas.

6. DISCUSSION

The measured temperature of N56-KT-7 indicate the inflow of surface water at elevations above 300 m, in contrast to the simulated temperature (Fig. 8). This discrepancy is attributed to insufficient data from the southwestern part of the analysis area, which prevents the accurate reproduction of the distribution of the low-permeability zone in this model.

Fig. 9 (v) shows the distribution of the low-temperature area in the southeastern and northwestern parts, indicating the existence of a hydrothermal system in the deeper eastern part of the analysis area. A previous study estimated the existence of a magma reservoir 2 km west of Onami-ike located in the eastern part of the analysis area (Yoshinaga et al., 2011), and this magma reservoir is the heat source for the formation of the hydrothermal system of western Kirishima Volcano.

From the temperature profile of N55-KT-1, the low-temperature zone extends deep underground (Fig. 8). Fig. 9 (vi) (a) shows that surface water penetrated deeper through the Sakkogawa fault. This result indicates that the Sakkogawa fault is the recharge zone of this geothermal area.

The hydrothermal fluids flow upward from depth (Fig. 9 (vi)), and flow from ENE to WSW directions through the Ginyu and Shiramizugoe faults (Figs. 9 (vii) and (viii)). This flow indicates that the reservoirs are formed along faults trending in the ENE-WSW direction. The formation of the high-temperature zone of 230 ℃ in the eastern part of the Ginyu fault indicates the presence of the Ginyu reservoir (Fig. 9 (b)). The permeability of the Ginyu fault is expected to be high owing to the constant temperature (Fig. 8). Additionally, a high-temperature zone of approximately 260 ℃ was formed in the eastern to central part of the Shiramizugoe fault,

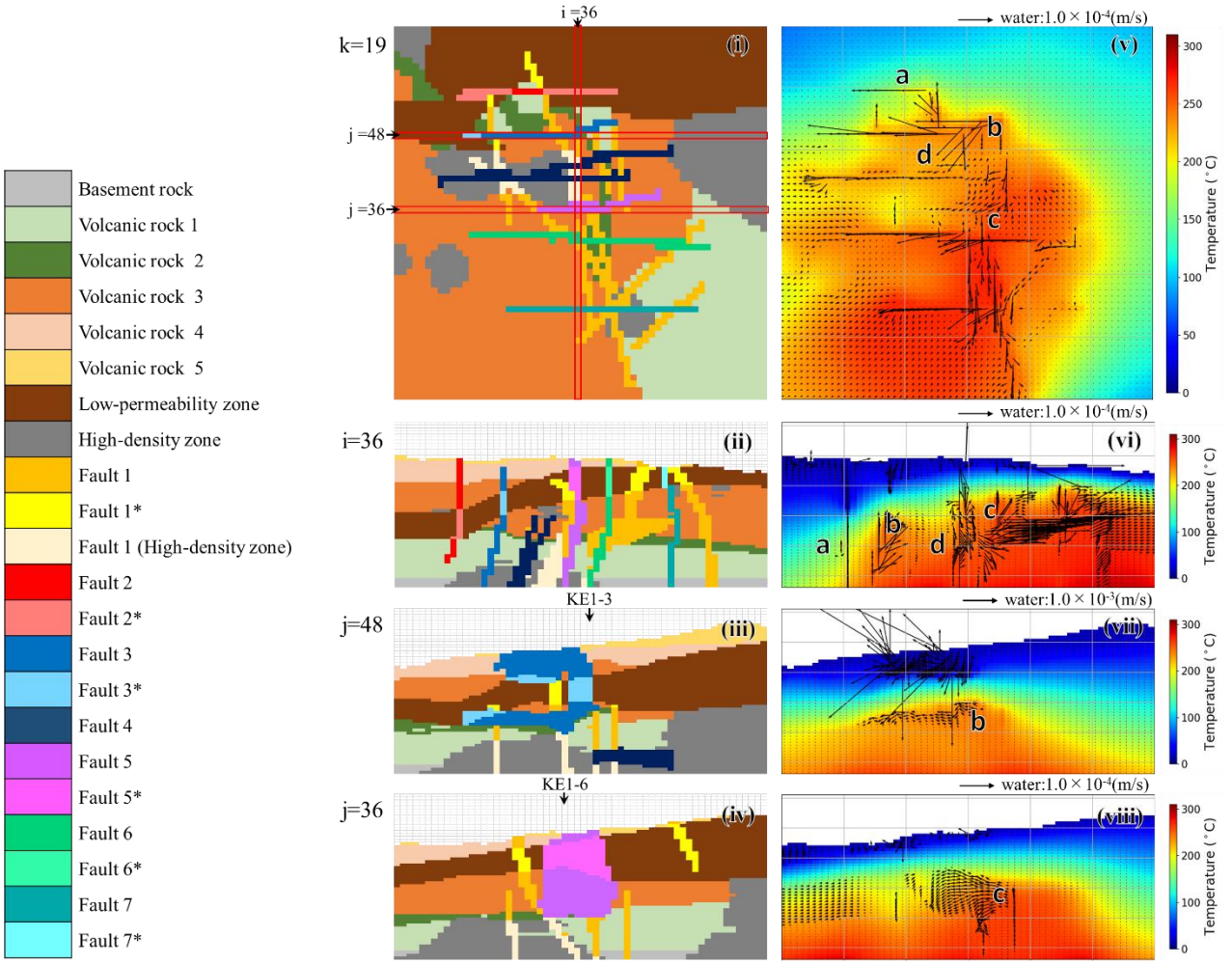

Figure 9: The left column indicates computational blocks in the horizontal view at -275 m a.s.l. (i), vertical section view in the NNW-SSE direction (ii), around Ginyu fault (iii), and Shiramizugoe fault (iv). The right column indicates the modeled temperature distributions and flow rates in the horizontal view (v), vertical section view in the NNW-SSE direction (vi), around Ginyu fault (vii), and Shiramizugoe fault (viii). *Low-permeability zone located at each fault.

indicating the presence of a promising geothermal reservoir (Fig. 9 (c)). This reservoir is expected to have high temperature and pressure.

Fig. 9 (d) shows the lack of flow between the Ogiri and Shiramizugoe areas. This result indicates that an impermeable layer exists between the Ogiri area in the northern part of the Kirishima geothermal area and Shiramizugoe area in the southern part. Therefore, the Ogiri and Shiramizugoe areas are likely independent of each other.

7. CONCLUSIONS

In this study, numerical simulations were conducted to elucidate the hydrothermal systems in the western part of Kirishima Volcano, and the following conclusions were obtained.

(1) The simulations were conducted using a model that included an impermeable layer estimated to exist between the Ogiri and Shiramizugoe areas. Consequently, the temperature profiles of the wells located in the eastern and central parts of the analysis area were reproduced well. Moreover, this model could reproduce the pressure difference between the Ogiri and Shiramizugoe areas by removing the influence of the groundwater surface. Therefore, this model reflects the actual subsurface structure well, with low permeability of the NW fault distributed in the high-density area between the Ogiri and Shiramizugoe areas.

(2) According to the simulation results, we inferred that geothermal reservoirs are formed by thermal water heated by magma reservoirs deep in the eastern part of the Kirishima area, rising through faults in the WSW-ENE direction. The high-temperature region of approximately 230 ℃ that formed along the Ginyu fault in the Ogiri district is the Ginyu fault. Additionally, a high-temperature zone of approximately 260 ℃ was formed along the Shiramizugoe fault in the Shiramizugoe district, indicating the existence of a high-temperature geothermal reservoir. These geothermal reservoirs are separated by an impermeable layer and are likely independent of each other.

(3) The simulation results showed good matching between the measured and calculated temperatures in the Ginyu and Shiramizugoe faults. However, those in some wells in the western region did not match well. As these wells appear to be an inflow of surface water, the distribution of impermeable layers in the western part of the analysis area must be considered.

ACKNOWLEDGEMENTS

We would like to express our deepest gratitude to Nittetsu Mining Co. for providing the data for this study.

REFERENCES

Goko, K., (2000). Structure and hydrology of the Ogiri field, West Kirishima geothermal area, Kyushu, Japan. Geothermics, 29, 127-149.

Ida, Y., Yamaguchi, M., and Masutani, F., (1986). Recent seismicity and stress field in the Kirishima volcano (in Japanese with English abstract). Bulletin Earthquake Research Institute, 39, 111-121.

Kagiyama, T., Ida, Y., Yamaguchi, M., and Masutani, F., (1990). Multi-active volcanic group generated in a slightly tensile stress field. Trans. American Geophysical Union 71, 964.

Kipp, K.L. Jr., Hsieh, P.A., and Charlton, S.R., (2008). Guide to the Revised Ground Water Flow and Heat Transport Simulator: HYDROTHERM–Version3. U.S. Department of the Interior, U.S. Geological Survey, Techniques and Methods 6-A25.

Middleton, M.F., (1979). A model for bottom-hole temperature stabilization. Geophysics, 44 (8), 1458-1462.

NEDO, (1983). Geothermal development promotion survey report, 3, Kurino-Tearai area (in Japanese). New Energy Development Organization, pp. 358-380.

NEDO, (1997). Geothermal development promotion survey report, C-1, Shiratori area (in Japanese). New Energy Development Organization, pp. 131.

NEDO, (2003). Geothermal development promotion survey report, C-4, Shiramizugoe area (in Japanese). New Energy Development Organization, pp. 199-201.

Nishijima, J., (2016). Density structure inferred from airborne gravity gradiometry survey data in the western part of Kirishima volcano (in Japanese with English abstract). BUTSURI-TANSA, 69 (1), 29-39.

Shimada, H., Fujimitsu, Y., and Nishijima, J., (2019). Geothermal Structure in the Western Part of Kirishima Volcano. Proceedings of International Symposium on Earth Science and Technology, 516-519.

Taguchi, S., Okaguchi, M. and Yamasaki, T., (1983). Fission-track Ages of Some Volcanic Rocks from the Kirishima Geothermal Region Report of Research Institute of Industrial Science. Kyushu Univ. 74, pp. 49-54.

Yoshinaga, K., Matsushima, T., Shimizu, H., Yamashita, Y., Yamazaki, K., Komatsu, S., and Fujiwara, S., (2023). Subsurface magma movement interred from extensometer and tiltmeter records during the early stage of the 2018 Shinmoe-dake eruptions, Japan. Earth, Planets and Space, 75, 143.